

COMPLEX WAVELETS AND ITS APPLICATION TO IMAGE FUSION

Xu Qing, Xing Shuai, Tan Bing, Li Jiansheng, Geng Zexun

Department of Remote Sensing Information Engineering, Zhengzhou Institute of Surveying and Mapping, No.66
Longhai Middle Road, 450052, ZhengZhou City, Henan Province, China-(xuqing_xingshuai@chxy.com)

Commission III, WG III/6

KEY WORDS: Algorithms, Multiresolution analysis, Image fusion, Multispectral, Remote sensing

ABSTRACT:

Image fusion deals with the integration of remote sensing images from various sensors, with multi-spectrum and high-spectrum, multi-angle viewing and multi-resolutions, aiming at achieving improved image quality to better support improved image classification, monitoring and etc. The main goal of this paper is to introduce a new approach to fuse panchromatic image and multi-spectral images by complex wavelet. First, the theoretical basis of complex wavelet is described together with its key properties(e.g. approximate shift invariance, good directional selectivity, perfect reconstruction(PR),limited redundancy and efficient order-N computation). Secondly, the new method for fusing remote sensing images based on complex wavelet is proposed. Finally experiment results show that the fusion method based on complex wavelet transform is remarkably better than the fusion method based on classical discrete wavelet transform.

1. INTRODUCTION

Image fusion deals with multi-sensors, multi-spectrum, multi-angle viewing and multi-resolutions remote sensing images from various, with, aiming at achieving improved image quality to better support improved image classification, monitoring and etc. Fused image will enhance reliability and speed of feature extraction, increase the usage of the data sets, and extend remote sensing images' application area. There have been a lot of research efforts on image fusion, and many fusion methods have been proposed. However, these image fusion methods are not enough and cause some difficulties for image analysis and application.

The advantages of wavelet transform is that it can analyze signal in time domain and frequency domain respectively and the multi-resolution analysis is similar with Human Vision System. The Discrete Wavelet Transform (DWT) in its maximally decimated form established by Mallat (S G Mallat, 1989) is widely used in image processing now. If we fuse a high resolution panchromatic image and a multi-spectral image by DWT, the fused image can conserve more spectral characteristics of the multi-spectral image. So the fusion method based on DWT is frequently used and become one of main fusion methods. But the DWT has two main disadvantages (N. Kingsbury, 1998a):

- Lack of shift invariance. This means that small shifts in the input signal can cause major variations in the distribution of energy between DWT coefficients at different scales.

- Poor directional selectivity for diagonal features, because the wavelet features are separable and real.

Nick Kingsbury has introduced the Dual-Tree Complex Wavelet Transform (DT CWT), which has the following properties (N. Kingsbury, 1998a):

- Approximate shift invariance;
- Good directional selectivity in 2-dimensions (2-D) with Gabor-like filters also true for higher dimensionality: m-D);
- Perfect reconstruction (PR) using short linear-phase filters;
- Limited redundancy: independent of the number of scales: 2:1 for 1-D ($2^m : 1$ for m-D);
- Efficient order-N computation - only twice the simple DWT for 1-D (2^m times for m-D);

The CWT has shown good performance in image restoration and denoising (A. Jalobeanu , 2000; Nick Kingsbury□1998b; Peter de Rivaz□2001), motion estimation (Julian Magarey□1998), image classification (Serkan Hatipoglu, 1999), texture analysis (Javier Portilla, 1999; N. Kingsbury, 1998; Serkan Hatipoglu, 1999), image enhancement (Nick Kingsbury□1998b), image matching (JIANG Han-ping , 2000).

In this paper, we propose a image fusion method based on CWT multi-resolution analysis. Experiment results show that the quality of fusion image based on CWT is better than fusion image based on DWT.

2. THE 1-D DUAL-TREE COMPLEX WAVELET TRANSFORM

It is well-known that the real biorthogonal wavelet transform can provide PR and no redundancy, but it is lack of shift variant. Then Kingsbury (Julian Magarey 1998; N. Kingsbury, 1998a ; Nick Kingsbury 1998b; Serkan Hatipoglu, 1999) has developed a dual-tree algorithm with a real biorthogonal transform, and an approximate shift invariance can be obtained by doubling the sampling rate at each scale, which is achieved by computing two parallel subsampled wavelet trees respectively.

For one dimension signal, we can compute two parallel wavelet trees. There is one sample offset delay between two trees at level 1, which is achieved by doubling all the sample rates. The shift invariance is perfect at level 1, since the two trees are fully decimated. To get uniform intervals between two trees beyond level 1, there have to be half a sample delay. The term will be satisfied using odd-length and even-length filters alternatively from level to level in each tree. Because we use the decimated form of a real discrete wavelet transform beyond level 1, the shift invariance is approximate.

The transform algorithm is described as following. Its process is illustrated by fig.1.

1D COMPLEX WAVELET TRANSFORM:

➤ At level 1, there is one sample offset between the trees.

$$\begin{aligned} (a_A^1)_n &= (a^0 * h^o)_{2n} & (d_A^1)_n &= (a^0 * g^o)_{2n} \\ (a_B^1)_n &= (a^0 * h^o)_{2n+1} & (d_B^1)_n &= (a^0 * g^o)_{2n+1} \end{aligned} \quad \square 1 \square$$

➤ Beyond level 1, there must be half a sample difference between the trees.

$$\begin{aligned} (a_A^{j+1})_n &= (a_A^j * h^e)_{2n} & (d_A^{j+1})_n &= (a_A^j * g^e)_{2n} \\ (a_B^{j+1})_n &= (a_B^j * h^e)_{2n+1} & (d_B^{j+1})_n &= (a_B^j * g^e)_{2n+1} \end{aligned} \quad \square 2 \square$$

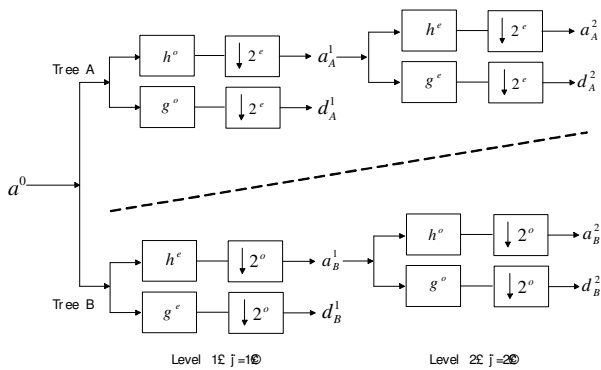


Figure 1. The unidimensional dual tree complex wavelet transform

The details d_A and d_B can be interpreted as the real and

imaginary parts of a complex process $z = d_A + id_B$. The essential property of this transform is that the magnitude of the step response is approximately invariant with the input shift, while only the phase varies rapidly (see (Nick Kingsbury 1998a) for a good illustration). (A. Jalobeanu, 2000)

It is not really a complex wavelet transform, since it does not use any complex wavelet. It is implemented with real wavelets. Classical complex-valued wavelet transforms can provide approximate shift invariance and good directionality, but PR and good frequency characteristics cannot be obtained using complex filters in a single tree. At the same time, it is different from a real wavelet transform because of the variety of filters. At level 1, the filter in tree A are odd-length filter, is same to tree B. Beyond level 1, the filters in two trees are different, and they are different between different levels in each tree. Hence the wavelet functions varies continuously from level to level, which is quite different from the classical multi-resolution analysis.

Reconstruction is performed independently in each tree, and the results are averaged to obtain a^0 at level 1, for symmetry between the two trees. This is illustrated by the following algorithm and fig 2.

1D INVERSE COMPLEX WAVELET TRANSFORM:

● Level j ($j > 0$):

$$\begin{aligned} (a_A^j)_n &= (\bar{a}_A^{j+1} * \tilde{h}^e)_n + (\bar{d}_A^{j+1} * \tilde{g}^e)_n \\ (a_B^j)_n &= (\bar{a}_B^{j+1} * \tilde{h}^e)_n + (\bar{d}_B^{j+1} * \tilde{g}^e)_n \end{aligned} \quad \square 3 \square$$

● At $j = 0$:

$$a_n^0 = \frac{1}{2} ((\bar{a}_A^1 * \tilde{h}^e)_n + (\bar{d}_A^1 * \tilde{g}^e)_n + (\bar{a}_B^1 * \tilde{h}^e)_n + (\bar{d}_B^1 * \tilde{g}^e)_n) \quad \square 4 \square$$

where $\bar{x}_n = \begin{cases} x_p & \text{if } n = 2p \\ 0 & \text{if } n = 2p+1 \end{cases}$, $\bar{x}_n = \begin{cases} x_p & \text{if } n = 2p+1 \\ 0 & \text{if } n = 2p \end{cases}$

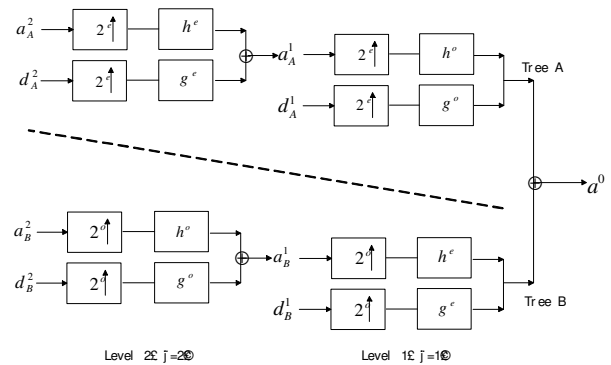


Figure 2. The unidimensional dual tree inverse complex wavelet transform

3. THE 2-D DUAL-TREE COMPLEX WAVELET TRANSFORM

For 2-D signals, we can filter separately along columns and then rows by the way like 1-D. Kingsbury figured out in (Nick Kingsbury [1998a]) that, to represent fully a real 2-D signal, we must filter with complex conjugates of the column and row filters. So it gives 4:1 redundancy in the transform. Furthermore, it remains computationally efficient, since actually it is close to a classical real 2-D wavelet transform at each scale in one tree, and the discrete transform can be implemented by a ladder filter structure.

The quad-tree transform is designed to be, as much as possible, translation invariant. It means that if we decide to keep only the details or the approximation of a given scale, removing all other scales, shifting the input image only produces a shift of the reconstructed filtered image, without aliasing. (A. Jalobeanu, 2000)

The most important property of CWT is that it can separate more directions than the real wavelet transform. The 2-D DWT produces three bandpass subimages at each level, which are corresponding to LH, HH, HL, and oriented at angles of 0° , $\pm 45^\circ$, 90° . The 2-D CWT can provide six subimages in two adjacent spectral quadrants at each level, which are oriented at angles of $\pm 15^\circ$, $\pm 45^\circ$, $\pm 75^\circ$. This is shown in fig 3. The strong orientation occurs because the complex filters are asymmetry responses. They can separate positive frequencies from negative ones vertically and horizontally. So positive and negative frequencies won't be aliasing. The orientations of details is shown in fig 4. Fig 5 shows the transform of an isotropic synthetic image at level 3, which also contains details at different scales. The orientation selectivity is more clear under each scale in comparison with the classical wavelet transform.

Since CWT has so many advantages, we consider use CWT to carry out image fusion instead of DWT. Then we design an image fusion method based on CWT in next section.

4. AN IMAGE FUSION APPROACH BASED ON CWT

The DWT has already been used for image fusion ten years ago. Though image fusion approaches by wavelet transform have been improved to be adaptive to process varied images, two disadvantages (lack of shift invariance and poor direction selectivity) still exist. They have hampered the further application of wavelet transform in image fusion.

The CWT is a good solution to this problem. It is approximate shift invariant. If the input signal shift a few samples, the fused image will be reconstructed without aliasing, which is useful to the not strictly registered images. Moreover it can separate positive and negative frequencies and provide 6 subimages with different directions at each scale. So the details of CWT can conserve more spatial information than DWT. The spatial

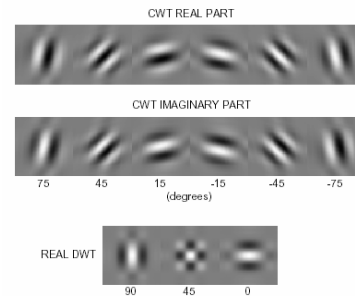


Figure 3. 2-D impulse responses of the complex wavelets at level 4 (6 bands at angles from -75° to $+75^\circ$) and equivalent responses for a real wavelet transform (3 bands)

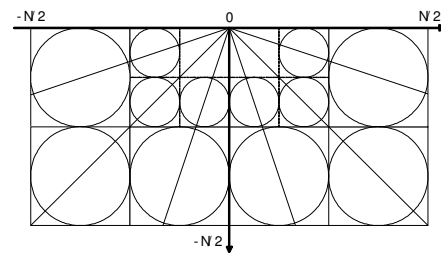


Figure 4. Directional selectivity of the frequency space corresponding to the complex wavelet transform



Figure 5. Left : isotropic test image containing various scale information, right: magnitude of its complex wavelet transform at level 3 showing both directional and scaling properties

can conserve more spatial information than DWT. The spatial resolution of the fused image is more closer to the high-resolution image. PR, limited redundancy and high computation efficiency make it suitable for image fusion.

We design an approach based on the quad-tree complex wavelet transform for fusing a low resolution multi-spectral image and a high resolution panchromatic image. First the registered multi-spectral image and panchromatic image are decomposed by complex wavelet respectively, then the approximate and detail parts of two images are fused according to some rule at each level, finally the fused image is reconstructed. This is illustrated by fig 6. The fusion procedure can be described detailedly as following:

- (1) Each band of the low resolution multi-spectral image and the high resolution panchromatic image are geometrically registered to each other. After geometrical rectification, the images have the same size.
- (2) The panchromatic image is stretched tally with each band of multi-spectral images respectively according to the histogram.
- (3) Decomposed the histogram-specified panchromatic image

and registered multi-spectral images with complex wavelet transform to form their multi-resolution and multi-directional descriptions. At the same time, the magnitudes of their complex wavelet transform are achieved.

(4) Image fusion begins with the coarsest level, the low frequency parts are replaced by the corresponding parts of multi-spectral images respectively. The high frequency parts at each scale cannot be replaced directly by the high frequency parts of panchromatic image, since the high frequency parts of the multi-spectral image don't only include spatial information, but also include spectral information. Considering that the complex wavelet transformation of the images can be interpreted as a complex process including real parts and imaginary parts and the magnitudes can show clear directionality, we fuse the high frequency parts according to the magnitudes. The details is illustrated in fig.6.

The wavelet coefficients at point (i, j) of real and imaginary parts in the high resolution image are denoted as $W_R^H(i, j)$ and $W_I^H(i, j)$ respectively. The wavelet coefficients at point (i, j) of real and imaginary parts in the low resolution image are denoted as $W_R^L(i, j)$ and $W_I^L(i, j)$ respectively. The magnitudes at point (i, j) in the high resolution image and the low resolution image are achieved respectively by

$$\begin{aligned} M^H(i, j) &= \sqrt{(W_R^H(i, j))^2 + (W_I^H(i, j))^2} \\ M^L(i, j) &= \sqrt{(W_R^L(i, j))^2 + (W_I^L(i, j))^2} \end{aligned} \quad \square 5 \square$$

The wavelet coefficient $CW(i, j)$ at point (i, j) in the fused image is obtained as following

$$CW(i, j) = \begin{cases} W^H(i, j) & M^H(i, j) \geq M^L(i, j) \\ W^L(i, j) & M^H(i, j) < M^L(i, j) \end{cases} \quad \square 6 \square$$

And then, the inverse wavelet transformations are carried out for composing the new merged images at this level.

(5) The replacement and composing procedure in (4) are carried out recursively at their top levels until the first level is processed. This results in three new images.

(6) The three new produced images are compounded into one fused image. The fused image does not only contain the spectral information content of original multi-spectral images and the structure information content of panchromatic image, but also enhance the original spectral and spatial information.

5. EXPERIMENTS

We chose two group images in experiments. One group includes a SPOT panchromatic image (acquired in 2002, ground resolution is 10 meters) and a Landsat7 TM multi-spectral image composed of 4th, 5th and 7th bands (acquired in 2000, ground resolution is 30 meters). The other

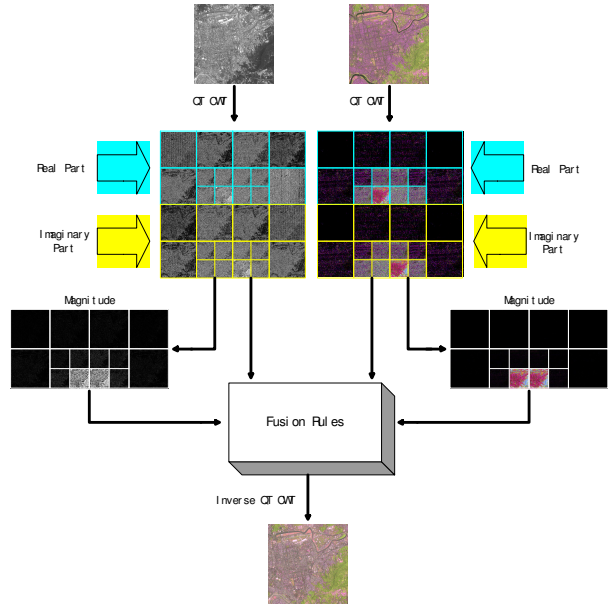


Figure 6. Procedure of image fusion based on complex wavelet transform

includes a IKONOS panchromatic image (ground resolution is 1 meters) and a IKONOS multi-spectral image (ground resolution is 4 meters), they are both acquired in 2003. The two groups of images are shown in fig 7 and fig 9. They have been registered strictly at the same scale. We fuse the images with different methods including direct power average, high pass filter, Intensive-Hue-Saturation (IHS) transform, DWT, discrete wavelet packet transform (DWPT). These images are used to compare with the image fused by CWT.

First we observe the fused images in fig 8 and fig 10. We find that (c) fully conserve spatial information of high-resolution image, but evident spectral distortion exist. The spatial resolution and spectral resolution of (a) and (b) have been improved limitedly. Then we find that the spectral characteristics of (d), (e), (f) are closer to the original multi-spectral image than other fused images. Among (d), (e) and (f), the spectral characteristic of (d) is closest to the original multi-spectral image, the spectral characteristic of (e) is similar with (f). Moreover, there is slight sawtooth in (d), (e), but (f) is perfectly smooth and clear. The discrete wavelet transform, discrete wavelet packet transform and complex wavelet transform are all carried out at two levels, therefore we can put them together for comparison.

Secondly we evaluate the performance of the fusion method based on complex wavelet transform using image quality indexes. The indexes we selected are average value, standard difference, entropy, average grads and fractal dimensions. Average value can show the distribution of the image grayscale in the rough. Standard difference and entropy can measure the information abundance in the image. Average grads shows exiguous contrast, varied texture characteristic and definition of the image. Fractal dimensions can describe the abundance degree of texture characteristics and the variety of pixel value in

the image. The statistics is shown in tab 1.

Table 1 shows that average value of fig 8(d) is closest to fig 7(b), fig 8(e) and fig 8(f) are very close to fig 7(b), but fig 8(c) is greatly different from fig 7(b). This demonstrates that the spectral characteristic of fig 8 (d) is closest to fig 7(b), the spectral characteristics of fig 8 (e) and fig 8 (f) are similar with fig 7(b). There is evident spectral distortion in fig 8(c). The conclusion accords with our observation. The statistics of standard difference and entropy show that spatial resolution of all the fused images have been improved, fig 8(c) is the clearest, fig 8 (f) is next best. Average grads and fractal dimensions of fig 8 (f) both are highest, since the details have been enhanced in fusion process, roads, bridges, airports, rivers and other objects are distinguished more easily.

Table 2 shows the result similar with table 1. Standard difference, entropy, average grads and fractal dimensions of fig 10 (f) all are highest, which shows obviously the details are enhanced. But the average value of fig 10 (f) is higher than other fused images except fig 10 (e), which demonstrates some distortions exist.

In a word, though there is slight spectral distortion in the fused image based on complex wavelet transform, it's spatial resolution and details texture have been enhanced remarkably. This demonstrates that the fusion method based on complex wavelet transform is better than the fusion method based on discrete wavelet transform and discrete wavelet packet transform.

6. CONCLUSIONS

In this paper, first we introduce a dual-tree complex wavelet transform with approximate shift invariance, good directional selectivity, PR, limited redundancy and efficient computation. Then we carry out image fusion using CWT instead of classical DWT, design a image fusion approach based on CWT. Experiment results show that the fusion method based on CWT is better than the fusion method based on DWT and DWPT.

REFERENCES

A. Jalobeanu , L. Blanc-Féraud , J. Zerubia□2000, Satellite

image deconvolution using complex wavelet packets□Thème 3— Interaction homme-machine,images, données, connaissances Projet Ariana Rapport de recherche n° 3955 —116 pages

Javier Portilla and Eero P. Simoncelli, 1999, Texture modeling and synthesis using joint statistics of complex wavelet coefficients, *Proceedings of the IEEE Workshop on Statistical and Computational Theories of Vision*, Fort Collins, CO, <http://www.cis.ohio-state.edu/~szhu/SCTV99.html>

JIANG Han-ping, WANG Jian-min, 2000, Application of Complex-valued Wavelet Transform to Image Matching, *Journal of Jiang-xi Institute of Education (Natural Science)*, Vol.21 No.6 , pp.29-31

Julian Magarey and Nick Kingsbury□1998, Motion estimation using a complex_valued wavelet transform□*IEEE Trans. on Signal Processing, special issue on wavelets and filter banks*, vol 46, no 4, pp 1069-84.

N. Kingsbury, 1998a, The dual-tree complex wavelet transform: A new technique for shift-invariance and directional filters, in *DSP Workshop*

Nick Kingsbury □ 1998b, The dual_tree complex wavelet transform: A new efficient tool for image restoration and enhancement□*Proc. European Signal Processing Conference, EUSIPCO 98, Rhodes*, pp 319-322.

Peter de Rivaz and Nick Kingsbury□2001, Bayesian image deconvolution and denoising using complex wavelets□*Proc. IEEE Conf. on Image Processing*, Greece, Oct 8-10, paper 2639.

Serkan Hatipoglu, Sanjit K. Mitra, and Nick Kingsbury, 1999, Texture classification using dual-tree complex wavelet transform, *IEE. Image Processing and its Applications*, Conference Publication No.465

S G Mallat, 1989, A theory for multiresolution signal decomposition: The wavelet representation, *IEEE Trans. PAMI*, 11(7), pp674-693

	Average Value	Standard Difference	Entropy	Average Grads	Fractal Dimensions
SPOT panchromatic image	130.327910	40.038097	6.987931	12.564874	2.952943
Landsat7 TM multi-spectral image	128.069414	23.931238	11.223637	4.046452	2.907271
direct power average	123.700075	21.678290	10.764350	5.870725	2.943095
high pass filter	123.699798	21.678528	10.764387	5.870922	2.943089
IHS transform	126.661916	43.560041	12.659949	13.679566	2.947926
discrete wavelet transform	127.556114	26.931699	11.492410	10.465421	2.956894
discrete wavelet packet transform	136.432717	24.632584	11.243407	8.922076	2.962865
complex wavelet transform	136.289744	28.501428	11.467674	12.921713	2.986830

Table 1. Statistics of quality indexes for evaluating the images in fig. 7 and fig. 8

	Average Value	Standard Difference	Entropy	Average Grads	Fractal Dimensions
IKONOS panchromatic image	55.003892	47.292947	6.971110	15.709922	2.950696
IKONOS multi-spectral image	54.959930	51.830456	12.012438	4.838858	2.881100
direct power average	52.168844	47.320513	11.948496	8.952973	2.915515
high pass filter	52.168796	47.320568	11.948493	8.952944	2.915515
IHS transform	54.500514	48.905712	11.558431	15.861264	2.948176
discrete wavelet transform	54.799508	54.022043	11.930620	15.345459	2.933445
discrete wavelet packet transform	62.241697	53.722484	12.253056	15.819710	2.935812
complex wavelet transform	62.211379	54.899634	12.175444	18.535382	2.949563

Table 2. Statistics of quality indexes for evaluating the images in fig. 9 and fig. 10

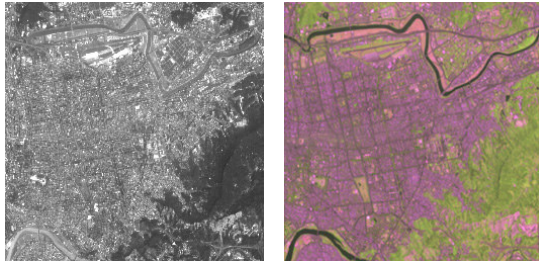


Figure 7. Left: SPOT panchromatic image, right: Landsat7 TM multi-spectral image composed of 4th, 5th and 7th bands



Figure 9. Left: IKONOS panchromatic image, right: IKONOS multi-spectral image

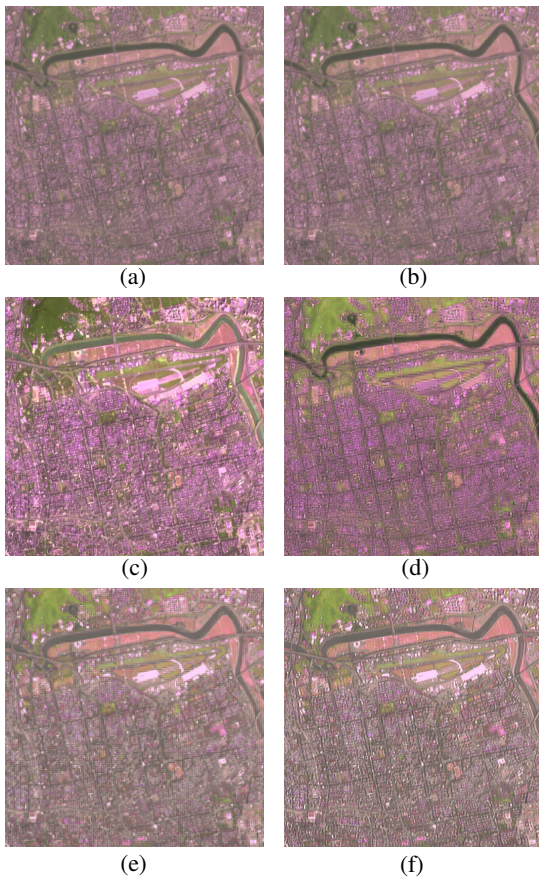


Figure 8. Fused images: (a) image fused by direct power average, (b) image fused by high pass filter, (c) image fused by Intensive-Hue-Saturation (IHS) transform, (d) image fused by discrete wavelet transform, (e) image fused by discrete wavelet packet transform, (f) image fused by complex wavelet transform

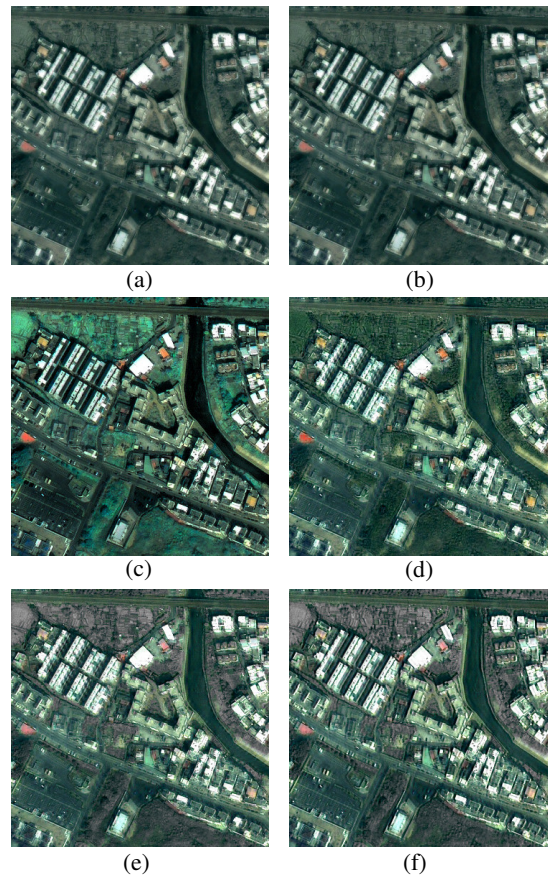


Figure 10. Fused images: (a) image fused by direct power average, (b) image fused by high pass filter, (c) image fused by Intensive-Hue-Saturation (IHS) transform, (d) image fused by discrete wavelet transform, (e) image fused by discrete wavelet packet transform, (f) image fused by complex wavelet transform